Journal Pre-proof

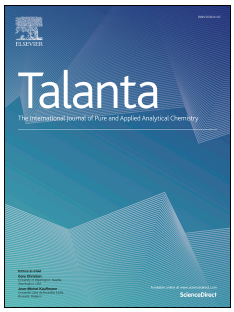

LDI-MS Scanner: Laser Desorption Ionization Mass Spectrometry-based biosensor standardization

Y.E. Silina, B. Morgan

PII: S0039-9140(20)30979-6

DOI: https://doi.org/10.1016/j.talanta.2020.121688

Reference: TAL 121688

To appear in: *Talanta*

Received Date: 17 July 2020

Revised Date: 15 September 2020

Accepted Date: 18 September 2020

Please cite this article as: Y.E. Silina, B. Morgan, LDI-MS Scanner: Laser Desorption Ionization Mass Spectrometry-based biosensor standardization, *Talanta*, https://doi.org/10.1016/j.talanta.2020.121688.

Yuliya E. Silina – was responsible for resources and funding acquisition, proposed conceptualization of presented research, development of the methodologies, investigation, validation, formal analysis and data visualization, project administration, performed writing original draft.

Bruce Morgan – was a part of project administration, reviewing & editing of the manuscript.

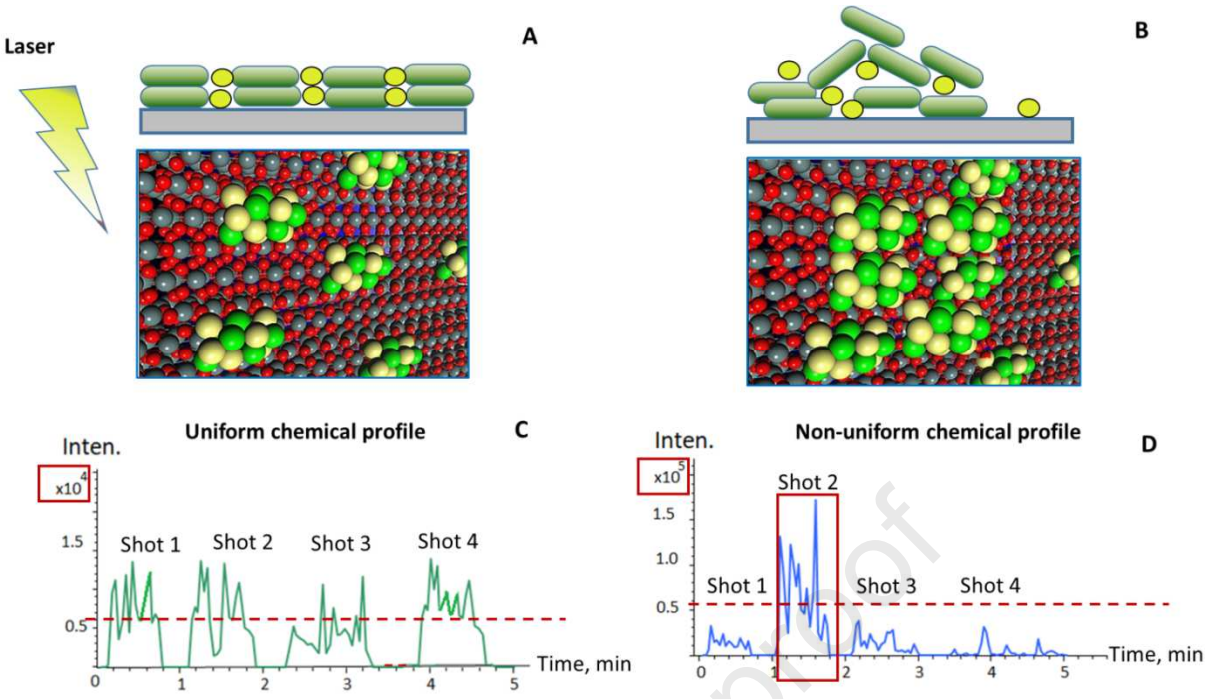

LDI-MS Scanner: Laser Desorption Ionization Mass Spectrometry-based biosensor standardization

Authors
Y.E. Silina*, B. Morgan

Institute for Biochemistry, Zentrum für Human und Molekularbiologie (ZHMB), Campus B 2.2, University of Saarland, 66123, Saarbrücken, Germany

*Corresponding author.
E-mail address: yuliya.silina@uni-saarland.de (Y.E. Silina)

Keywords
Biosensors, Nanobiosensors, Standardisation, LDI-MS, Biochemical profiling, Quality control

Abstract

Amperometric biosensors have been widely utilized for the cost-effective and rapid analysis of various bioanalytes, for example glucose. However, a lack of standardization and validation procedures remains a major limitation in biosensor development. Therefore, despite rapid advances in material science driving the development of amperometric biosensors, to date only a few biosensors, detecting a limited range of analytes, are available on the market. It is believed, once this issue is addressed, it can significantly facilitate the next step in the overall concept "go to the market" production and implementation of amprerometric biosensors for a large industrial scale.

Herein, we report on the use of laser desorption ionization mass spectrometry (LDI-MS) for the standardization of amperometric biosensors, based upon a complete and non-destructive characterization and validation of layer by layer (LbL) biosensors at each fabrication step. We reveal that specific ionization pathways of mediators, polymers and enzymes from the biosensor surface allows for robust quality control during LbL biosensor manufacture. Furthermore, this LDI-MS approach can also be used to monitor, and therefore ensure, the encapsulation of enzymes in one-step designed nanobiosensors. Specifically, we show that LDI-MS can be used for the rapid chemical profiling of LbL biosensors and one-step synthesized nanobiosensors, as well as to assess their synthesis quality and to monitor for batch-to-batch and intra- and inter- day changes in their function and behavior. Our novel approach will thus contribute to the future development, improved design and fine tuning of both conventional LbL-fabricated amperometric biosensors and one-step designed nanobiosensors.

1. Introduction

Progress in material science in general and specifically in the development of organic-inorganic (O-I) hybrids has driven rapid advances in many areas, including point-of-care measurement systems, biosensors, nanoreactors and metabolic analysis.[1] Notably, in metabolic analysis, the targeted biomolecules are often present at very low concentrations (i.e. ng/μL level). Furthermore, detection can be impeded by the presence of interfering species. Therefore, there has been increasing interest in the use of laser desorption ionization mass spectrometry (LDI-MS), together with novel O-I materials, which can promote desorption-ionization, as a powerful new approach for metabolic analysis.

O-I hybrids are self-assembled systems consisting of inorganic (metal/semiconductor/dielectric particle or bulk component) and organic components, such as polymers, enzymes, antibodies, DNA or amino acids. Such O-I materials come in numerous forms including porous, micro- and nano-structured substrates. In principle, LDI-MS, utilizing O-I substrates, enables high-sensitivity, high-resolution, high-

throughput, accurate and easy-to-perform analyses, for example in hospitals.[2,3] However, to date, this approach has not been widely accepted in routine laboratories due to a range of problems including high background, as well as low sample-to-sample and spot-to-spot reproducibility.

Remarkably, similar problems also beset biosensors based upon O-I hybrids. Thus, only a few biosensor designs have left the research laboratory and been introduced on the market. One explanation for this situation is a lack of standardization procedures as well as poor validation and metrology of the O-I hybrid materials used for biosensor development. For example, without the use of robust nanoanalytical methods for the characterization of O-I hybrids, the percentage of each ligand present in the organic component can only be estimated based upon the material ratio used in the synthesis reaction. In addition, modern biosensors regardless of the read-out platform (amperometric, potentiometric or photoluminescence detection) suffer from low sensor-to-sensor and batch-to-batch synthesis and signal reproducibility. [4,5,6,7–9]

A wide spectrum of quality control methods can be used to characterize the individual organic bio-receptor, or inorganic components of O-I hybrids.[10] However, none of the existing analytical methodologies, used in isolation, allow for the complete characterization of O-I hybrids, i.e. amperometric biosensors.

In this study we adapted an LDI-MS- based approach, originally developed and widely used in the context of bioanalytical chemistry, as a tool for standardization of layer-by-layer (LbL) designed amperometric biosensors and one-step fabricated nanobiosensors (as a case study). We demonstrate rapid and non-destructive characterization of amperometric LbL biosensors at each fabrication step, including monitoring of mediator (Prussian Blue), immobilization of enzyme (glucose oxidase, GOx) and Nafion layer formation used to protect bioreceptor (GOx) from elution.

In addition, by utilizing LDI-MS as a biochemical scanner, we demonstrate the possibility for ensuring the encapsulation of GOx in one-step designed nanobiosensors produced from multicomponent electrolyte solution contained palladium nanoparticles (Pd-NPs), Nafion and enzyme. This study is expected to improve our understanding of the surface chemistry of amperometric biosensors and also will provide an opportunity to improve their design and fine tune their performance.

2. Materials and Methods

2.1 Materials

H_2PdCl_4, $(NH_4)_2HPO_4$ and $Na_2HPO_4{\cdot}12H_2O$ used for Pd-electrolyte preparation were of 99 % purity (Sigma Aldrich), Flavin adenine dinucleotide disodium salt hydrate (FAD, 99.7%), BSA (5% v/v), Glucose oxidase (GOx) from *Aspergillus niger* (EC 1.1.3.4, type VII, 248 U/g solid) were obtained from Merck (Darmstadt, Germany). Glutaraldehyde solution (25% (v/v)), ethanol (UV HPLC gradient, 99.9%), H_2O_2 solution (30% (v/v)), potassium hexacyanoferrate (III) (ACS reagent, ≥99.0%), iron (III) chloride (anhydrous, 99.99%), D-Glucose (anhydrous) and Nafion®117 solution (~5% (v/v) in a mixture of aliphatic alcohols and water) were obtained from Merck (Darmstadt, Germany). The DRP-110DGPHOX screen printed electrodes (SPEs) were provided by DropSens (Llanera, Spain). The electrodes were printed on ceramic substrate and each sensor consists of a carbon working electrode (WE) modified with graphene oxide (GO) layer, a carbon counter electrode and a silver reference electrode. All the solvents were of HPLC quality. Organic-free, deionized (DI) water was generated by an Elga PureLab (Celle, Germany) water purification system.

2.2 Prussian blue (PB) film preparation

The preparation of Prussian Blue (PB) films used for biosensing applications was described in previous studies.[11] Briefly, 10 µl of freshly prepared precursor solution, containing 0.1 M potassium ferrocyanide ($K_3[Fe(CN)_6]$) in 10 mM HCl was mixed with 0.1 M ferric chloride ($FeCl_3$) solution in 10 mM HCl (1:1 proportion (*v/v*)) directly over the WE surface (GO) of the SPEs electrodes. To stabilize the formed PB layer, the sensors were placed in an oven at 100 °C for 2 h. All the PB modified GO/SPEs were stored in the dark with humidity ≤ 60% prior to the subsequent microscopic, electrochemical and mass spectrometry studies.

2.3 Layer-by-layer (LbL) biosensor fabrication (approach 1 and approach 2)

The LbL procedure for biosensors fabrication was reported earlier with some modification implemented here.[12] Briefly, on a PB modified GO/SPE electrode a 2.5 µL droplet of freshly prepared glutaraldehyde solution (1% (v/v) was placed and left to dry at the ambient conditions for 20-30 min. Afterwards, individual GOx and Nafion layers were deposited in a multi-step manner according to the following procedure: 3µl of GOx dissolved in phosphate buffer and BSA (5% v/v) was placed over the PB and glutaraldehyde modified GO/SPE followed by deposition of 3 µL of Nafion®117 (2.5% v/v in EtOH). The finalized biosensors consisted of 4 layers which were referred to as *approach 1*.

To compare the analytical merit of the above described 4 layered biosensors (*approach 1*) and one-step nanobiosensors (see below), freshly mixed GOx solution dissolved in phosphate buffer and BSA was mixed with Nafion®117 (2.5% v/v in EtOH) in a 1:1 ratio and deposited over the PB and glutaraldehyde modified GO/SPE electrode with a volume of 3 µL. The finalized biosensors consisted of 3 layers and were referred to as *approach 2*. All the prepared biosensors were placed to dry overnight in a climate chamber at 40% humidity and 8 °C regardless of the employed preparation protocol.

2.4 One-step designed nanobiosensors (approach 3)

One-step fabrication of nanobiosensors with encapsulated GOx and Nafion®117 was carried out at room temperature 20±2°C directly over the surface of GO/SPE according to the previously reported protocol.[12] The synthesis was performed in one-step from the multiple electrolyte solution (containing Pd-electrolyte, Nafion®117 (2.5% *v/v* in EtOH) and GOx dissolved in phosphate buffer and mixed in the ratio of 1:1:1 *v/v/v)* in chronopotentiometric mode on the one-channel biologic Potentiostat PalmSens4 (PalmSens, Utrecht, Netherlands) at the current density of 2.5 mA and deposition time of 30 sec. The process results in the formation of the hybrid Nafion-doped Pd-NPs with encapsulated GOx. This preparation route was fully controlled by the PSTrace Software (PalmSens, Utrecht, Netherlands). The fabricated one-step designed nanobiosensors (referred to as *approach 3*) were washed with DI water and stored in the dark.

2.5 Electrochemical characterization of LbL biosensors and one-step designed nanobiosensors

The electrochemical response of PB-modified electrodes, LbL biosensors (*approach 1* and *approach 2*) and one-step designed nanobiosensors (*approach 3*) were recorded in cyclic voltammogram (CV) mode on the one-channel biologic Potentiostat PalmSens4 (PalmSens, Utrecht, The Netherlands) at the scan rate of 20 mV/sec. The amperometric response during calibration of nanobiosensors (*approach 3*) was recorded using the same type of potentiostat in the microanalytical range of glucose from 0 to 40 µM at the applied voltage equal to −0.08 V. All measurements from the same nanobiosensor were recorded at least in triplicate.

2.6 Laser desorption ionization mass spectrometry (LDI-MS)

LDI-MS investigations of the fabricated PB-based biosensors, LbL biosensors (*approach 1* and *approach 2*) and one-step designed nanobiosensors (*approach 3*) were carried out on a Bruker Esquire 3000+ESI-ion trap MS (Bruker Daltonics, Bremen, Germany) operated by Bruker esquire control 5.3 software equipped with atmospheric pressure AP-MALDI ion source and Nd:YAG solid-state laser (355 nm, Frequency 200 Hz, 3 ns, laser fluence 45%, 12000 laser shots per spot). The studied sensors were adapted directly onto the conventional MALDI plate followed by subsequent analysis according to the algorithm of LDI-MS, Figure S1. Mass spectra were recorded in both positive and negative detection modes in the range of *m/z* 100-1000. TIC and EIC chromatograms were used for data analysis.

2.7 PB biosensor performance by oxygen release studies

To estimate the impact of PB layer homogeneity on the biosensor performance, the dynamic response of the oxygen release rates following the reaction between H_2O_2 and PB was measured. To this end, an OXR430 retractable needle-type fiber-optic oxygen minisensor (Pyro Science GmbH, Aachen, Germany) coupled to a FireStingO2 fiber-optic meter (Pyro Science GmbH, Aachen, Germany) was used.[13] The oxygen minisensor was controlled by the Pyro Oxygen Logger software. The response of the fiber-optic oxygen minisensor was recorded in oxygen release mode (µmol/L) based on (1):

$$PB(_{red}) + H_2O_2 \rightarrow PB(_{ox}) + H_2O + O_2\uparrow \quad (1)$$

2.8 Enzyme activity measurements prior and after LDI-MS studies

To verify the enzyme activity (GOx as a case study) during immobilization in biosensor layer before and after LDI-MS studies (*see above*), an OXR430 retractable needle-type fiber-optic oxygen minisensor (Pyro Science GmbH, Aachen, Germany) was utilized. The response of the minisensor was recorded in the oxygen consumption mode (µmol/L) according to the sequences (2-3):

$$\text{Glucose} + GOx(_{ox}) \rightarrow GOx(_{red}) + \text{Gluconic acid} \quad (2)$$

$$GOx(_{red}) + O_2 \rightarrow GOx(_{ox}) + H_2O_2 \quad (3)$$

To measure the enzyme activity in a droplet after immobilization, the tip of the optical minisensor was placed perpendicular to the WE of GO/SPE electrodes. The stable signal of the dissolved oxygen was obtained and recorded when simultaneously 150 µL of analyte (glucose solution in phosphate buffer, pH=7) was placed over all three electrodes and the potential of the redox reaction was applied (i.e. amperometric characterization) to the synthesized LbL biosensors (*approach 1* and *approach 2*) or one-step designed nanobiosensors (*approach 3*) connected to a single Potentiostat PalmSens4 (PalmSens, Utrecht, The Netherlands).

2.9 Scanning Electron Microscopy (SEM)

SEM images were captured on a Quanta 400 FEG system (Hillsboro, OR, USA) equipped with an EDAX (Mahwah, NJ, USA) Genesis V 6.04 X-ray spectral analysis system, at an accelerating voltage of 10 keV.

3. Results and Discussion

3.1 Non-destructive screening of film chemical homogeneity

Quantification of hydrogen peroxide (H_2O_2) within biological or clinical samples is a challenging analytical task. The conventional H_2O_2 detection methods such as colorimetry, spectrophotometry, chromatography, chemiluminescence suffer from poor reliability, reproducibility, low selectivity and sensitivity.[14] In addition, the above mentioned techniques can be very time consuming. Biosensors have overcome these limitations due to their simplicity, high sensitivity, selectivity and rapidity.

Prussian Blue (PB) is one of the most studied sensitive layer which has been successfully employed in layer by layer (LbL) designed biosensors due to its selective ability towards H_2O_2 decomposition.[13] A wide spectrum of approaches with different rates of success was used to prepare PB films on the surface of working electrodes. However, regardless of the fabrication protocols used, in order to maintain reliable H_2O_2 quantification, it is highly important to control the entire PB preparation route.[15,16,17]

Remarkably, numerous techniques can be employed to investigate the properties of PB on an electrode surface. For example, the morphology of PB films is characterized by scanning electron microscopy coupled with X-ray analysis (SEM/EDX) and the surface roughness is routinely studied using atomic force microscopy (AFM). To investigate the electrochemical response obtained from PB-based biosensors, cyclic voltammetry (CV) or amperometry (AM) can be used. Nonetheless, appropriate methods for evaluating the chemical homogeneity and for visualizing the chemical profile of PB have been lacking. This is important as the chemical homogeneity of PB can dramatically affect biosensor performance, i.e. intensity and reproducibility of the obtained response as well as signal-to-noise ratio.

Whilst several mass spectrometry-based assays for the detection of PB in historical pigments and artworks have previously been developed[18,19] these approaches required destructive preparation steps, for example pre-treatment of the PB containing layer with NaOH or suspension in either water or linseed oil resulting in the detection of ion species that are mostly attributable to the matrix. Therefore, the development of alternative mass spectrometry-based approaches for analysis of PB layer in its pristine form would be highly desirable. The usage of a "soft" ionization mass spectrometry approach, viz. laser desorption ionization mass spectrometry (LDI-MS) for non-destructive testing of PB on an electrode surface can be considered as a possible solution to the problem.

Usually, in LDI-MS development, the targeted analyte is spotted on the surface of the functional substrate (including porous silicon, graphite, graphene nanoparticles, metal nanoparticles or nanostructured coatings, etc.[20,21,22,23]). This is followed by its desorption, ionization and subsequent MS analysis . In this case, the surface of the substrate serves as a donor of H^+, Na^+, K^+ ions (positive ionization mode) or electrons (negative mode) which are necessary to provide an effective ionization of the analyte. Notably, the working electrode (WE) of a SPE is covered by graphene oxide (GO) as a sensitive element responsible for the transport of electrons. GO has been approved as a promising substrate for LDI-MS analysis of numerous bioanalytes, i.e. carbohydrates, long-chain fatty acids, triacylglycerols, flavonoids and phenylpropanoids. In this regard, it can be hypothesized that similar to biomolecules, the efficient laser induced desorption and ionization of the PB layer from the surface of a GO modified SPE can occur. Once this hypothesis is confirmed it will allow to use of LDI-MS screening of PB-based biosensors.

First, as a proof-of-principle, we screened the chemical homogeneity of PB films directly on the surface of a GO/SPE, without any sample pretreatment procedure. The general concept for estimating of the chemical homogeneity is illustrated in Figure 1, A,B. Thus, a chromatogram obtained from a chemically uniform layer during laser shot will give rise to equal intensity analytical signals (Figure 1, C). In contrast, sufficiently different MS-signal intensities with "spike-like" effect (Figure 1, D) extracted from the chromatograms can be used to infer a chemically heterogeneous profile. The underlying principle is similar to the "sweet spot" phenomenon usually seen in MALDI-MS and caused by formation of non-homogenous and different polymorphous crystal structures by a dried-droplet preparation

method. Thus, as a result of macrocrystal formation, different efficiency of analyte ionization followed by large variation in MS-signal intensity can be established.[24,25] With regards to our concept towards estimating the chemical homogeneity of the biosensor layer, the "spike-like" effect is minimized or less pronounced in case of a chemically uniform layer (Figure 1, C). Therefore, to distinguish the uniform and non-uniform film formation, the absence of a clear "spike-like" effect in chromatogram profile can be readily used as criteria.

Remarkably, the degree of the chemical homogeneity/inhomogeneity of PB film and the defined acceptable threshold values can be readily found on the next step (if necessary) depending on the synthesis protocol used (drop casting or electrodeposition of PB) or customer product requirements.

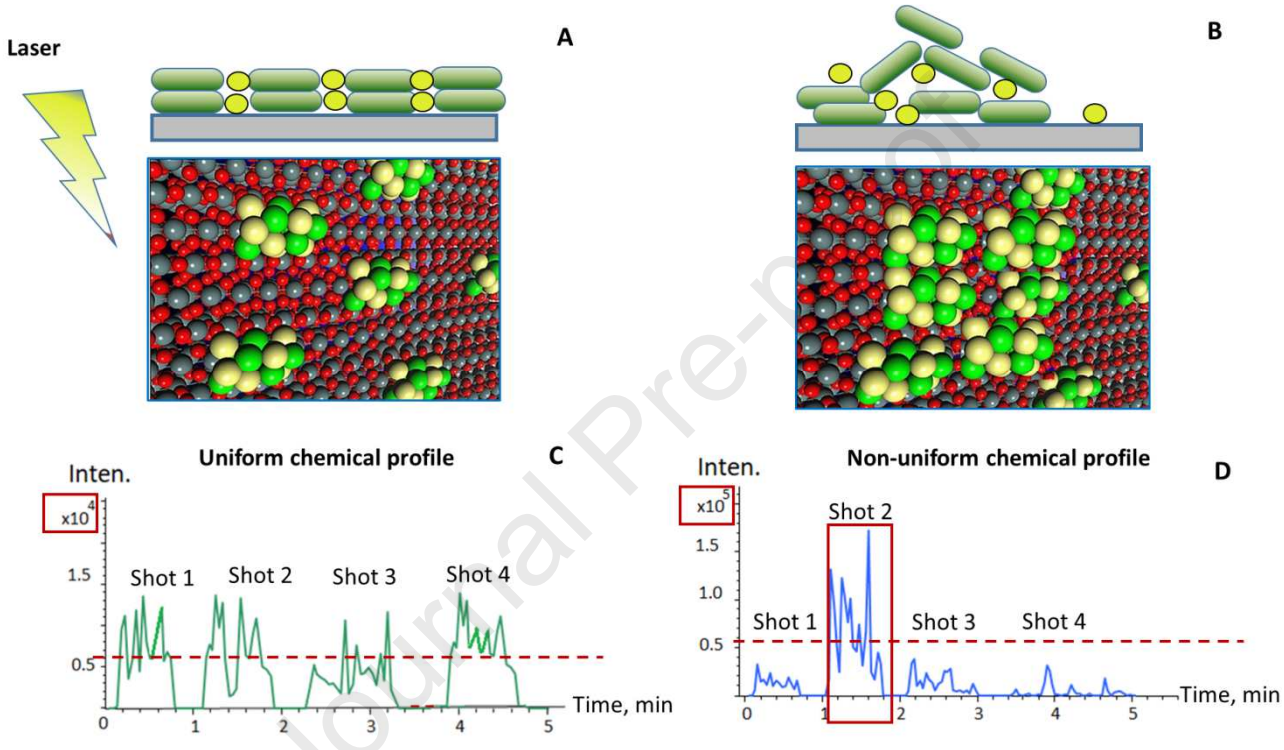

Figure 1 – Schematic illustration of LDI-MS platform applied for validation of PB-based biosensors with uniform (A) and non-uniform (B) chemical profiles (top). TIC chromatograms received from biosensors with uniform (C) and non-uniform/spiked (D) (bottom) profile. Dash line (C, D) – acceptable thresholds values (defined upon the requirements of analytical task, viz. linearity range, LOQ, LLOQ, etc).

However, to achieve this ambitious goal, the identification of characteristic ionic species obtained from PB modified GO/SPE is a first step towards visualization of the film chemical homogeneity. In previous studies employing mass spectrometry-based approaches (ESI-MS) for the analysis of PB layer in historical pigments and artworks, the extensive decomposition of PB seen at *m/z* 107.9 ($[Fe(CN)_2]$-), *m/z* 133.9 ($[Fe(CN)_3]$-) and *m/z* 159.9 ($[Fe(CN)_4]$-) was reported.[11,18,19,26] Nonetheless, in our experiments utilizing "soft" ionization technique (LDI), the decomposition of PB was not confirmed. Thus, the most stable and abundant peaks for PB layer were found at *m/z* 165.8, 189.7 and 241.7 which were attributed to the presence of $Fe(OCN)_2(CN)$-, $Fe_2(CN)_3^-$ and $Fe_2(CN)_5^-$, respectively (Figure 2 A,C). Moreover, LDI mass spectra obtained from PB modified GO/SPE biosensors in negative ionization mode mostly exhibited by repeatable adducts with a mass of 26 Da (replacement of CN-) and 24 Da (CN-2ē). We hypothesize that the formation of these unusual patterns can be attributed to the specific electron transfer between the GO and PB layer.

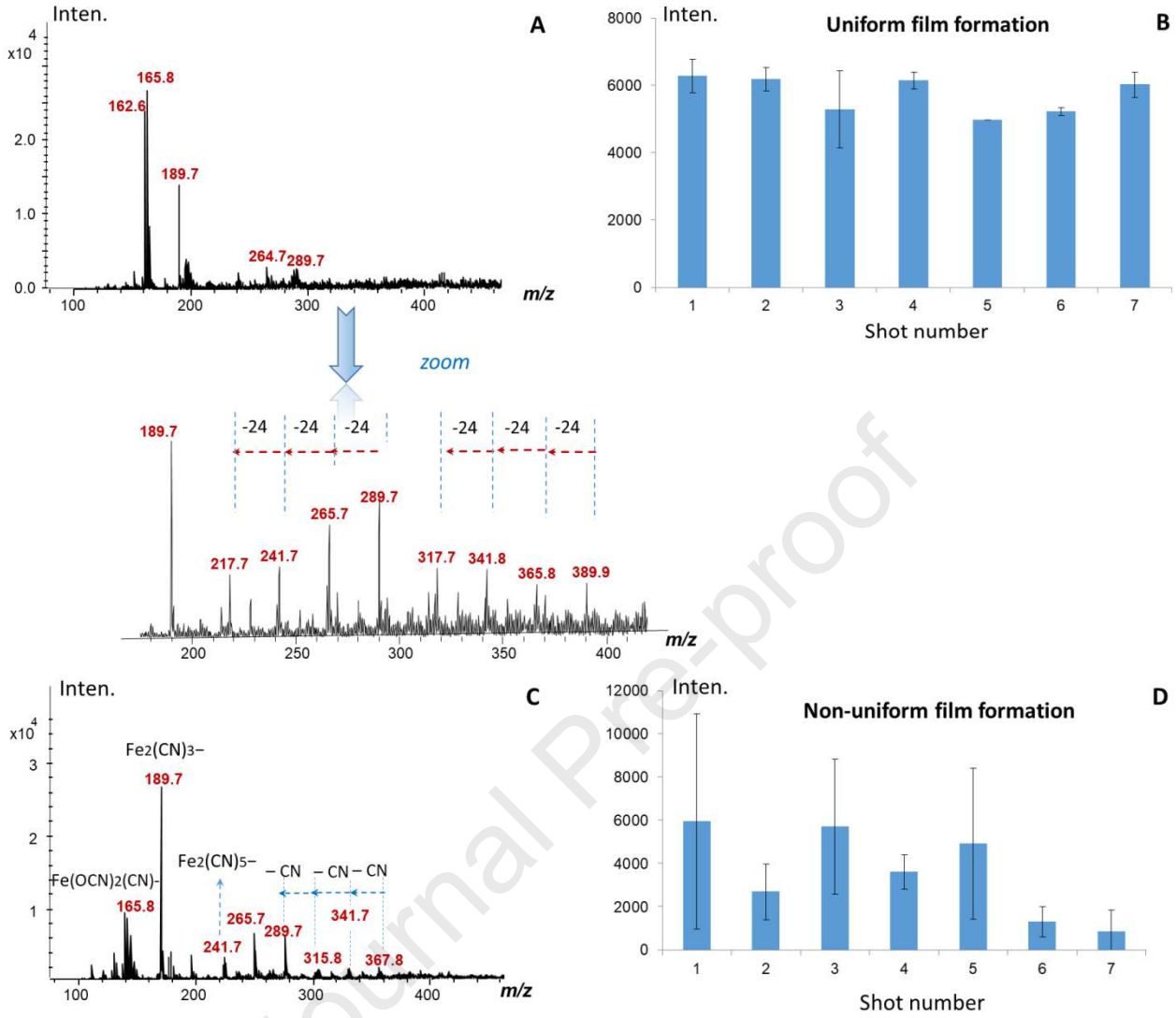

Figure 2 – LDI mass spectra (A,C) obtained from uniform (A) and non-uniform/spiked (C) PB modified GO/SPE in negative ionization mode. (C,D) – dependency of extracted signal intensity (monitored at *m/z* 189.7) obtained from PB/GO/SPE on shot number. Note: The measurement shown in (B,D) were repeated in triplicate.

Next, the defined ionization pathway for PB layer formed on the surface of GO/SPE was used to test the homogeneity/inhomogeneity of a PB-based biosensor. To this end, the most environmentally stable peak at *m/z* 189.7 was extracted from the chromatogram and monitored (Figure 2B,D). We studied two independent PB films prepared by a conventional drop casting approach (*see Experiment*). Surprisingly, different LDI-MS readout signals were recorded highlighting a different distribution of PB from the two films despite the use of identical Prussian Blue solutions and identical synthesis conditions. As a consequence, different analytical performance of these PB-based biosensors might be expected *a priori* resulting in the low sensor to sensor signal reproducibility. This expectation was confirmed by oxygen minisensor studies based on the testing of PB films with peroxide. We observed that the catalytic activity of PB-biosensors towards peroxide decomposition for the uniform film was much higher as compared to the non-uniform film (Figure 3). This can be explained in terms of improved transport phenomenon within the uniform PB film resulting in the superior interaction between H_2O_2 and PB layer. In contrast, the formation of non-uniform PB islands (see Figure 1,B) can significantly impede the penetration of H_2O_2 through the sensitive mediator layer and limit the overall decomposition of analyte.

The results of the oxygen minisensor studies performed for these PB-films can be used as indirect evidence for their different chemical profiles previously revealed by LDI-MS. Notably, this oxygen minisensor assay can also be considered as a crucial and informative approach towards control of PB preparation route. At the same time, the testing of PB-based biosensors employing peroxide and an oxygen minisensor was destructive in nature (*non-destructive "no"/informative tool "yes"*). This was confirmed by subsequent electrochemical and LDI-MS studies (Figure S2). Thus, a significant lost in electrochemical activity of the PB film, as well as a strong difference in mass spectra as compared to non-tested films was established. This indicates a complete degradation of PB layer after contact with peroxide (ESI, Figure S2, *bottom*). However, non-destructive SEM studies of the PB layer before and after the testing with peroxide did not reveal any changes in the surface morphology of the film (Figure S3). Therefore, SEM cannot be considered as a crucial and informative approach towards screening of PB layers (*non-destructive "yes"/informative tool "no"*).

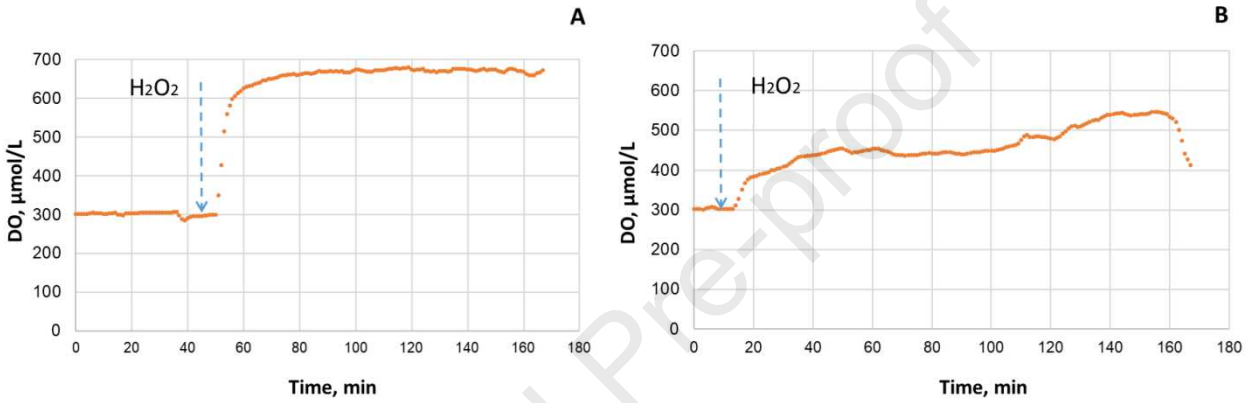

Figure 3 – Dynamic response of the oxygen release rates (dissolved oxygen, DO, µmol/L), during the reaction between uniform (A) and non-uniform (B) films of PB with 10 mM of peroxide. Note: the experiments were performed at room temperature, 20±2 °C.

In contrast to the oxygen minisensor profiling of PB-biosensors , the optimized LDI-MS assay and the defined pattern route applied for the screening of chemical homogeneity of PB films was non-destructive in nature. Furthermore, no differences were recorded from PB/GO/SPE in CV experiments allowing us to rule out possible melting or sintering effects caused by the laser ,[27] which were previously reported for metal-based micro- and nano- dimensional structures after laser irradiation, , Figure S4. This result confirms a "soft" ionization of PB layer from the surface of GO/SPE and preservation of its pristine form (*non-destructive "yes"/informative tool "yes"*). In contrast, CV studies usually used for biosensors characterization, whilst a powerful and informative analytical tool, has been reported as a destructive approach (*non-destructive "no"/informative tool "yes"*).[11]

We next utilized LDI-MS to monitor the changes in PB-based biosensor storage conditions. Different top ionic species were recorded from PB-biosensor kept with exposure to ambient light for 5 days indicating the degradation of the intact sensitive layer, see ESI, Figure S5.

In summary, we revealed a novel pathway of PB ionization in LDI-MS and showed that this data can be utilized to monitor changes in a preparation route of PB-biosensors as well as during their experimental use (see Figure S2,B) or storage conditions (Figure S5). Remarkably, LDI-MS used for the screening of PB-based biosensors offers several advantages over alternative mass-spectrometry techniques, for example (*i*) the possibility to analyze the biosensor surface in its pristine form, (*ii*) the received ion species can be

exclusively attributed to the targeted layer of biosensor instead of the used template/target (Au-plate, paper) or matrix (*i.e.* linseed oil)[18,19] (*iii*) the assay is non-destructive in nature and therefore allows further usage of biosensor.

3.2 Towards imaging the chemical profiles of biosensors

Nafion®117 (further referred to as Nafion) is frequently used in biosensors to protect water soluble enzymes from elution. Typically, , Nafion is employed as the last/top layer in LbL designed biosensors. To fabricate the Nafion protective membrane, several physical (drop casting) and electrochemical approaches resulting in the formation of layers with a different thickness can be used.[11] Remarkably, the thickness of the polymer layer can dramatically affect the permeability of Nafion-based membrane, its diffusion properties, transport behavior and thus, the entire LbL biosensor response and its analytical performance. For example, a significant difference in the biorecognition mechanism between several Nafion multi-layered biosensor architectures by oxygen and glucose monitoring in a droplet was reported.[11] In addition, different performance (limit of detection, standard deviation, storage time, etc) and mechanical stability of "two" and "four" Nafion-based layered biosensors were revealed by tandem of several methods, viz. inductively-coupled plasma mass spectrometry (ICP-MS), liquid chromatography-electrospray ionization-tandem mass spectrometry (LC-ESI-MS/MS) and electrochemical studies (AM).[11] Although, the above-mentioned tandem monitoring used for tracking of the impact of biosensor design on its analytical performance is a promising and comprehensive analytical approach, it can be very time consuming. Moreover, once the optimal design is established, the quality control of the biosensors at the development stage to facilitate the overall concept "to the market" production would be highly desirable.[10]

To further explore the possibilities of LDI-MS as a crucial quality test, we were thus interested to apply this approach to screen the Nafion layers on the surface of biosensors dependent of their architecture. To this end, LbL biosensors (prepared according to *approach 1* and *approach 2*; *see Experiment*) and one-step designed nanobiosensors (*approach 3*) were tested without any sample pretreatment procedure. Surprisingly, we detected different ionic species from LbL biosensors depending upon their fabrication protocol (*approach 1 or approach 2*) (Figure 4).

Thus, for LbL biosensors fabricated according to *approach 1*, a clear release of repeatable $C_4F_5^-$ species was observed, regardless of the ionization mode (see also Figure S6). In contrast, LDI-MS spectra obtained from LbL biosensors prepared by *approach 2* exhibited $CF2^-$ repeatable ions. This result can be explained by a different thickness of the Nafion membrane/film (*approach 1* involves a 4-layered design; *approach 2* involves a 3-layered architecture). Remarkably, determination of the top ion peaks associated with a certain tested layer is the main challenge with respect to the imaging of LbL biosensors. For instance, different types of reference ions can be generated from LbL biosensors employing Nafion-based membrane and tested in a liquid state, i.e. $CF_3COO_2^-$ (*m/z* 112.9870), $C_8HF_{14}O_2^-$ (*m/z* 394.9780), $CF_3(CF_2)_4CF_5CFCF_2COO_2^-$ (*m/z* 424.9921), $CF_3(CF_2)_4CF(COOH)COO_2$ (*m/z* 388.9697) species.[28] However, the usage of the wrong characteristic species for standardization of biosensors, i.e. evaluation of their preparation routes, can be fatal in terms of metrology.

Interestingly the unusual pathway of Nafion ionization from the surfaces of GO/SPE following the release of repeatable characteristic small monomers from the polymer framework was in line with previously reported dependency found by LDI-MS for Triton X-100 deposited on the solid surface with silver nanoparticles. Briefly, release of repeatable characteristic fragments $(-[C_2H_4O]^-$units) by 44 atomic mass units according to their degree of ethoxylation corresponding to Triton X-100 was detected.[10] Thus, the application of LDI-MS methodology and obtained knowledge on laser desorption/ionization routes for a wide range of polymers employed as protective membranes in biosensor development followed by formation of the specific database can significantly gain the quality test during production of amperometric biosensors with different architecture and type of the protective membrane.

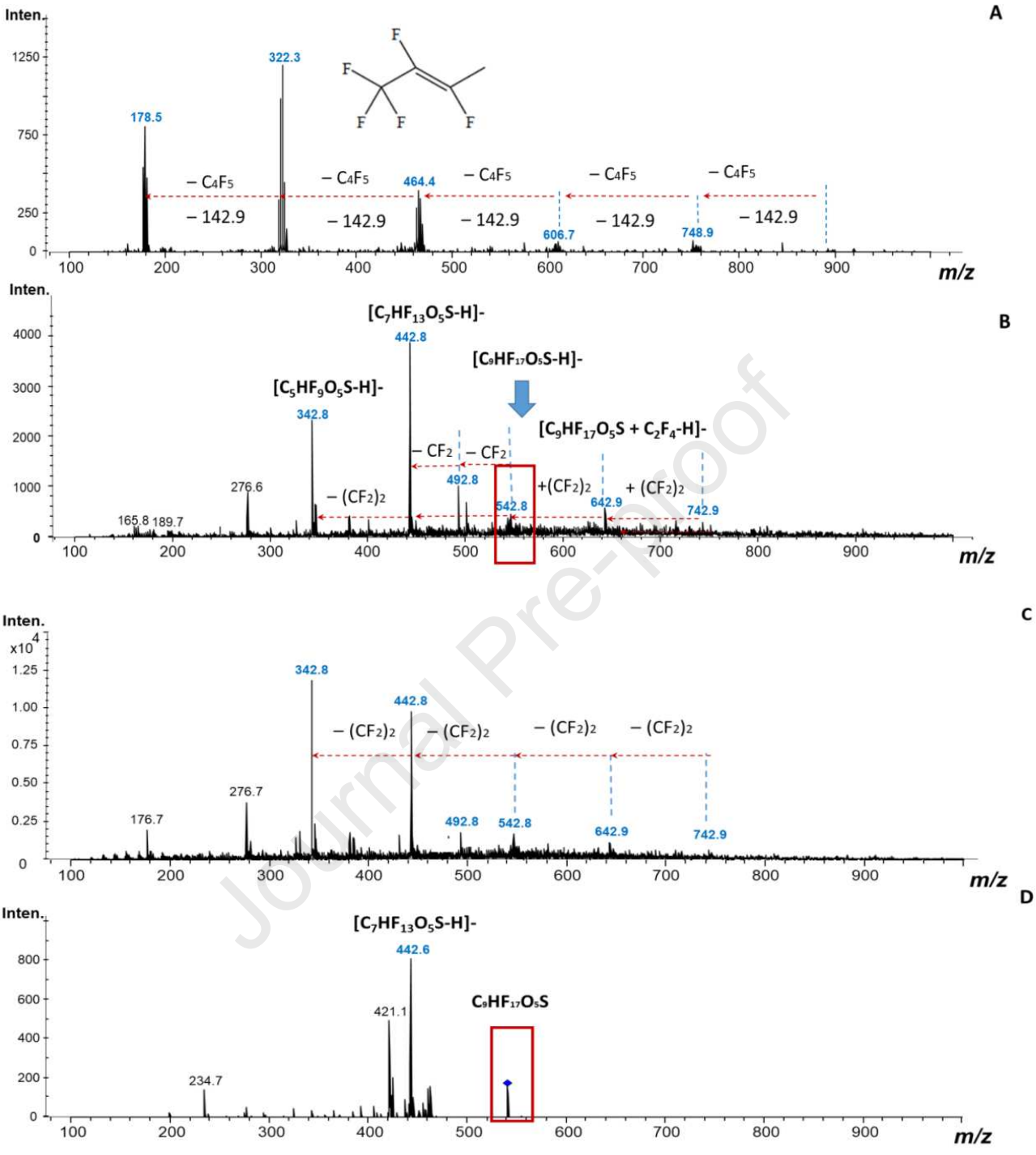

Figure 4 – TIC mass spectra (A-C) obtained in negative detection mode from LbL biosensors produced by *approach 1* (A), *approach 2* (B), and one-step designed nanobiosensor, *approach 3* (C). (D) MS^2 spectra of *m/z* 542.8 recorded from (C). Note: all experiments were performed at least in a triplicate with the same results.

Importantly, the fact that we detected various Nafion species from differently prepared LbL biosensors by LDI-MS was essential because the thickness of the polymer membrane film and its distribution over the surface of GO/SPE results in the different transport behavior of analyte and therefore, affects the overall sensor response. Thus, this parameter (polymer distribution, thickness and homogeneity of the

layer) should be particularly controlled during LbL biosensor fabrication. However, CV investigations revealed almost no change in behavior of these LbL biosensors (Figure S7). At the same time, despite the similarity of CV responses obtained from tested LbL biosensors (Figure S7), the biorecognition mechanism in these multi-layered structures can be very different.[11] In summary, CV studies might be not such an informative tool towards screening of the design and preparation routes of LbL biosensors, i.e. membrane architecture and thickness. In contrast to CV investigations, LDI-MS assay allowed reliable and visible tracking of LbL biosensors preparation routes (see Figure 4,A,B).

To further validate our results, we performed similar LDI-MS experiments to screen the Nafion architecture on the surface of one-step designed nanobiosensors (*approach 3*). Surprisingly, almost identical top ionic species were found in the mass spectra received from nanobiosensor as recorded from the surface of LbL biosensor prepared by *approach 2* (Figure 4C). It was unexpected because such a different one-step preparation route should result the formation of Nafion-doped nanoparticles (*approach 3*) with a thinner and single layer as compared to three layered architecture (*approach 2).*

To clarify this question, quantification of the deposition rates of Nafion layer formed by *approach 2* (layered architecture) and by *approach 3* (NPs-based architecture) was performed. For this goal, a series of Nafion calibration solutions in the range of 200 – 20000 ppm were prepared and deposited over GO/SPEs surfaces followed by LDI-MS analysis based on *m/z* 542.8 as the most stable peak (Figure 4D). Notably, the deposition of Nafion by *approach 3* was only possible in the presence of Pd-electrolyte resulting in the formation of Nafion-doped Pd-NPs. The concentration of calibrants for deposition of Nafion (*approach 3)* has been adjusted to take into account the presence of Pd-electrolyte (in the same range as for a*pproach 2).* Each calibrant solution was individually dropped (*approach 2)* or electroplated (*approach 3)* on the surface of GO/SPEs resulting in the formation of 10 biosensors and 10 nanobiosensors followed by their subsequent analysis according to algorithm of LDI-MS.

Interestingly, we observed a strong quantitative difference in the top ion species corresponding to Nafion for these tested systems, Table 1. The efficiency of Nafion deposition rates by means of *approach 2* (layered architecture) was found to be very low as compared to *approach 3* (NPs-based architecture), i.e. 11% versus 78%, respectively. The low deposition value (an approx. 11%) of Nafion membrane prepared by means of dropping over the surface of GO/SPE (*approach 2*) also explains the similarity in mass spectra received from this LbL biosensor and mass spectra obtained from one-step designed nanobiosensor (*approach 3).* We assume, that low deposition rates of Nafion for biosensor prepared by *approach 2* can be explained by chemicals solubility difference, spreading and evaporation effects which take place during dropping of Nafion solution over surface of GO modified SPEs. These effects can be minimized by electroplating in one-step designed nanobiosensors (*approach 3), see Experiment*.

Table 1 – Assay data (n = 10) for Nafion deposition rates (laser fluence 45%). Data extracted from full scan spectra

Fabrication approach	Calibration formula	R^2	DR*, ng/spot	E**, %
LbL biosensor, approach 2 (layered architecture)	y =2.7681x + 10423	0.9803	350±17	11.29
One-step designed nanobiosensor, approach 3 (NPs-based architecture)	y = 0.052x – 3.3333	0.9995	676±23	78.07

*DR – deposition rates found based on calibration curve; **E – efficiency of deposition.

Besides different deposition rates of Nafion, diverse EIC chromatograms from LbL biosensor (*approach 2*) and one-step designed nanobiosensor (*approach 3*) were obtained as well (ESI, Figure S8). The continuous chromatographic peaks in EIC negative ionization mode with a similar distribution over the scanned period from nanobiosensor (*approach 3*) as compared to non-regular zigzag shapes recorded from LbL biosensor (*approach 2*) for Nafion characteristic species were received. Moreover, the chromatographic peak quality (frequency of the repeatable characteristic peaks, S/N ratio) supplied by one-step designed nanobiosensor (NPs-based architecture) was much higher as compared to LbL analogues. The observed result can be readily explained in terms of homogeneously distributed hybrid O-I nanoparticles contained Nafion (Nafion-doped Pd-NPs) over the surface of nanobiosensor. Thus, the presence of NPs in the nanobiosensor design can result into the advanced desorption/ionization of Nafion during interactions with UV-laser.[29] Therefore, EIC chromatograms recorded from the biosensor prepared by *approach 2* (layered design) and *approach 3* (NPs-based architecture) can significantly help to establish even a minor qualitative or quantitative difference in their design, validate their preparation routes, improve the quality control tests at the development stage and permit rational design. This opens up the possibility for fine imaging and tuning of the studied systems.

In conclusion, LDI-MS profiling of Nafion layer performed directly on the surface of GO/SPE allows completely avoiding the chemical usage and waste generation. Moreover, this methodology can be readily extended to non-enzymatic biosensors based on the usage of polymer-based membranes to circumvent electroactive interferents frequently seen in environmental and medical samples.

Based on the LDI-MS results obtained above, the term "LDI-MS scanner" applied for validation of biosensors and nanobiosensors will be further used.

3.3 LDI-MS scanner to ensure enzyme encapsulation in nanobiosensors

To test whether a LDI-MS used as a 'scanner' can support the entire preparation route in biosensors and nanobiosensors development, including the screening of bio-receptor, we applied the above described experiments for analysis of the enzymatic layer. Regardless of the preparation approach (LbL or NPs-based architecture), only presence of the specific bio-receptor (enzyme) can guarantee a reliable, sensitive and selective response of biosensor. Thus, numerous of non-enzymatic biosensors with a low cost, high stability, quick response, and low detection limit via direct electrochemical oxidation of electroactive bioanalytes (glucose, lactate, dopamine, choline, serotonin, acetylcholine, etc.) were introduced.[30,31,32,33,34] However, non-enzymatic biosensors are unsatisfactory with regards to the targeted analyte selectivity in real samples. Moreover, they suffer from matrix interference and show quick loss of activity during reaction. Therefore, selective detection of electroactive bioanalytes in real matrices is still possible only by means of employment of the specific enzymatic reaction.

Remarkably, the manufacturing of a one-step designed nanobiosensor (*approach 3*) relies on a simultaneous encapsulation of enzyme (GOx) with Nafion and Pd-NPs from a phosphate multiple electrolyte on top of the sensor surface (*see Experiment*). However, to the best of our knowledge, there is still no analytical technique which can be used to ensure the successful enzyme co-deposition/encapsulation from the complex electrolyte solution. Thus, AM studies exclusively based on the obtained calibration curves cannot always be considered as a helpful tool to guarantee the presence of the dropped or encapsulated enzyme in biosensor architecture. The obtained AM response can be simply generated as a result of a direct electrochemical oxidation occurred in a manner similar to non-enzymatic biosensors behavior, for example, due to the presence of Pd-NPs. In this regard, LDI-MS 'scanner' can serve as a desirable alternative to ensure enzyme encapsulation via co-deposition or to get closer insights into the functionality of one-step designed nanobiosensors (*approach 3*).

To address this question, we studied LDI-MS response obtained from the bio-receptor component in nanobiosensor(*approach 3*). Primarily, it was important to find out the top ions species which could be associated with GOx. Surprisingly, mass spectra recorded from the surface of nanobiosensor exhibited by numerous water clusters (18 amu), see Figure 5 A. This observation was important because the amount of the water retained in the enzyme structure can directly correlate with its catalytic activity. Moreover, the presence of water in the enzymatic nets determines the environmental stability of biosensors, their storage and shelf time. This fact was highlighted in several studies.[35,36] In other words, with LDI-MS scanner we visualized and approved the presence of water in one-step designed hybrid nanobiosensors (*approach 3*) that can explain their previously observed advanced analytical performance.[12]

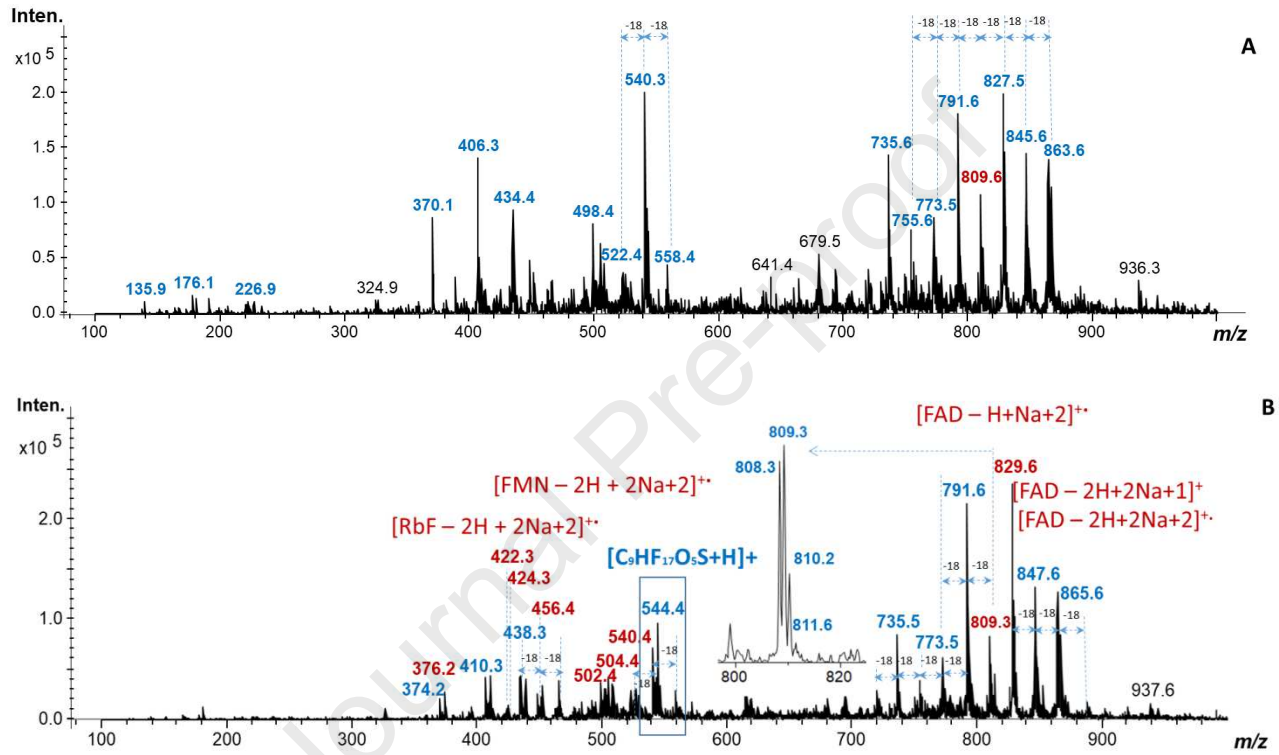

Figure 5 – TIC spectra obtained in positive ionization mode from (A) one-step designed nanobiosensor with encapsulated GOx (*approach 3*); (B) one-step designed nanobiosensor with encapsulated FAD (250 ng/µL) in the presence of interfering Nafion species. Note: all experiments were performed at least in triplicate with the same results.

Another important result observed in this set of experiment was a high similarity of the obtained LDI-MS spectra with a spectrum typical for the individual flavin adenine dinucleotide (FAD) employed as a co-factor in GOx preparation route (Figure 5). In contrast to the large proteins (~ 80 kDa) present in GOx, FAD is a small molecular weight organic compound which can be readily desorbed and ionized in LDI-MS similar to the process which occurs in ESI-MS or matrix assisted laser desorption ionization mass spectrometry (MALDI-MS).[37]

Next, to verify the obtained ionic species from one-step designed nanobiosensor to encapsulated GOx/FAD, a droplet of pure GOx was spotted on the surface of GO/SPEs and analyzed by LDI-MS. Interestingly, the same types of characteristic ionic patterns were recorded from the dropped GOx-modified GO/SPEs which were received from the nanobiosensor (*approach 3*), see Figure S9. This simple experiment can be considered as a proof for successful encapsulation of GOx (monitored as a co-factor) in one-step designed nanobiosensor (*approach 3*).

Furthermore, the encapsulation of the individual FAD molecule from multicomponent (FAD, Nafion, Pd-electrolyte) solution was performed. This experiment allows us for a better visualization and identification of the ionic species recorded from the hybrid one-step nanobiosensor. Interestingly, FAD was reduced in positive-ion resulting in the formation of abnormal spectral behavior on LDI-MS. That is, in addition to the expected [M+H]+, [M+Na]+, the unusual [M-H+Na]+, [M-H+Na+1]+, [M-H+Na+2]+., [M-2H+2Na]+, [M-2H+2Na+1]+, [M-2H+2Na+2]+· species were detected, Figure 5B. Moreover, the formation of the similar ion species of the smaller flavins, i.e. flavin mononucleotide (FMN) and riboflavin (RbF) with water clusters and clear transfer of even numbers of electrons was observed. It is assumed that the mechanism behind this reaction is similar to what occurs in the biological redox systems, rather than the transfer of hydrogen.

Further, due to the complexity of the resulting mass spectra received from the hybrid nanobiosensor (*approach 3*) the most important step was to correctly determine the top ion peaks associated with Nafion and encapsulated GOx. To define all the observed species to the certain substance, encapsulation of the individual GOx and Nafion with Pd-NPs was carried out. Figure S10 shows the individual accessory of the observed multiple ion species in Figure 5A. Thus, a simple comparison of these individual mass spectra allowed to clearly identifying the top characteristic peaks received from the hybrid one-step designed nanobiosensor (*approach 3*).

In addition, as we mentioned at the begging of this section, the difference in responses of non-enzymatic (pure Pd-NPs or Nafion-doped Pd-NPs nanobiosensors) and enzyme-based nanobiosensors (*approach 3*) is not always clearly seen by means of AM studies. In other words, pure Pd-NPs (without encapsulated GOx) can also lead to the transformation of glucose to gluconic acid via electron transfer resulting in the current (AM signal) appearance in a substrate (glucose) concentration dependent manner. To exclude these speculations, we need to guarantee encapsulation of enzyme with Pd-NPs and Nafion during fabrication of one-step designed nanobiosensors. This is readily possible to perform by means of comparison of the reference mass spectra obtained from pure Pd-NPs or Nafion-doped Pd-NPs and mass spectra recorded from one-step designed nanobiosensor (see ESI, Figure S10). Therefore, LDI-MS screening allows to avoid time and chemicals consuming CV and AM studies which can only indirect approve the presence of enzyme by performing of series reproducible calibrations in a specific concentration range (μM-mM) of the substrate.

To conclude, LDI-MS scanner allowed visualization of each layer of the conventional LbL-designed biosensors: from PB film distribution (inorganic component) and Nafion layer (organic component) screened in negative detection mode to GOx (bioreceptor) monitored in positive ionization mode. Each layer produces very different mass spectra, TIC or EIC chromatograms with the characteristic ion species. In this regard, LDI-MS scanning can be readily considered as a quality test for fabrication of conventional LbL biosensors and one-step designed nanobiosensors. More importantly, the discovered here ionization pathway of enzyme from the surface of one-step nanobiosensor represents a new route for quality control in their manufacturing.

3.4 Towards the guidelines for the standardization of biosensors and nanobiosensors

Last, the impact of laser treatment on the electrochemical response of one-step nanobiosensor (*approach 3*) and its enzymatic activity was evaluated. Notably, CV studies did not reveal any changes in nanobiosensor potential and its electrochemical behavior if the laser was applied to the surface no longer than 45 sec (Figure 6).

Note that even a longer laser treatment during 180 sec applied to nanobiosensor surface did not result in a significant loss in enzymatic activity (Figure 7). Thus, even at these non-optimal experimental conditions (180 sec vs 45 sec, was applied to make the trend pronounced) more than 75% from the intact enzyme activity retained preserved. At the same time, the treatment of the surface during 45 sec was enough to distinguish the difference between the chemical profiles of nanobiosensors and LbL analogues. Thus, the continuous chromatographic peaks in EIC mode with a similar distribution over the scanned period from nanobiosensor surface as

compared to non-regular zigzag shapes recorded from LbL-designed biosensor were received (Figure S11). In addition, the chromatographic peak quality with respect to its location in the chromatogram and reported analytical information supplied by the nanobiosensor was much higher versus LbL analogues. This phenomenon can be attributed to the presence of Pd-NPs in the architecture of one-step designed nanobiosensors.[29]

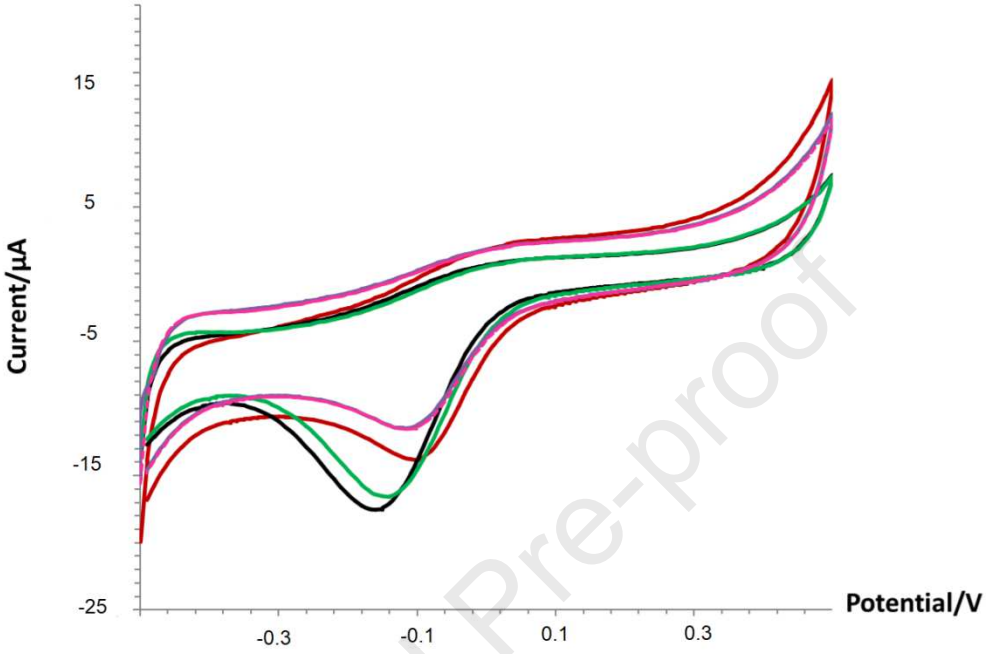

Figure 6 – Cyclic voltammograms recorded in phosphate buffer at 20 mV/sec scan rates from nanobiosensor based on Pd-NPs (*approach 3*) with encapsulated Nafion and GOx before (**blue** line) and after LDI-MS studies: **pink** (dash line) – laser was applied for 45 sec; **red** – laser applied for 60 sec; **green** line – laser applied for 120 sec; **black** – laser applied for 180 sec. A slight shifting in a potential (green and black lines) is explained by possible melting/sintering effect of Pd-NPs[27] which can occur after the laser treatment.

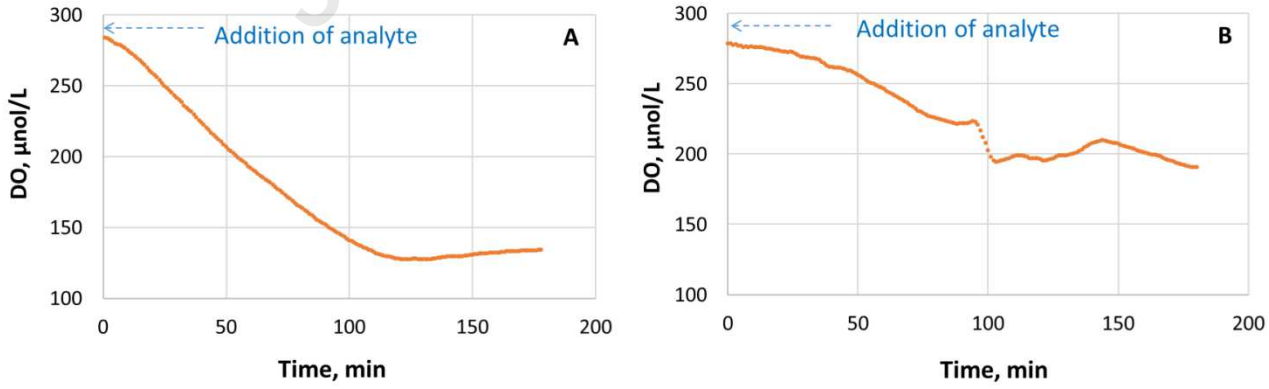

Figure 7 – Dynamic response of the oxygen consumption rates (dissolved oxygen, DO), expressed as the numbers of moles (µmol/L) produced during reaction between analyte (glucose solution, 1 mM) and one-step fabricated nanobiosensor (*approach 3*) before and after LDI-MS studies performed during 180 sec. Laser fluence 45 %.

To this end, such informative chromatograms recorded from the nanobiosensors during only 45 sec can help to establish even a minor qualitative or quantitative difference in their design. Remarkably, the industrial nanometrology requires rapid both qualitative and quantitative (see section "*Towards imaging the chemical profiles of biosensors*", Table 1) measurements with a minimal number of the controlled parameters. In this regards, the screening of one-step designed nanobiosensors by LDI-MS scanner during only 45 sec would be a possible solution.

Further, evaluating the potential of LDI-MS platform as a rapid tool/scanner for the validation of one-step nanobiosensors, i.e. sensor to sensor behavior was studied. Despite a very similar chemical profile recorded in TIC mode during first 45 sec (Figure 8) for two nanobiosensors from the same batch, a clear difference in EIC mode was detected, Figure S12. This result can be readily interpreted in terms of a minor difference in a surface chemistry of one-step fabricated nanobiosensors (*approach 3*).

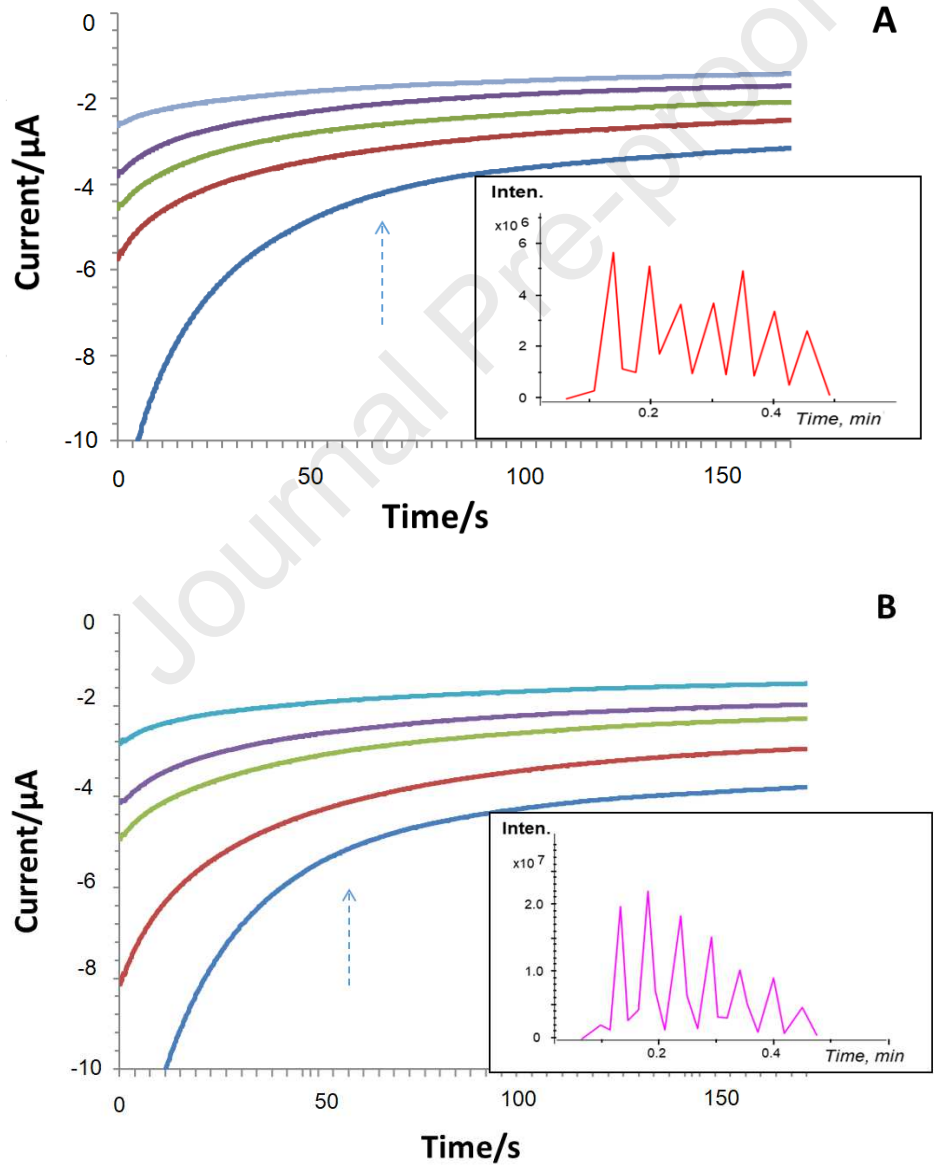

Figure 8 – AM calibration curves (A,B) received from nanobiosensor 1 (A) and nanobiosensor 2 (B) from the same batch at pH=7. Insert - TIC spectra (obtained in positive ionization mode from the same batch of nanobiosensors (*approach 3*): (A) nanobiosensor 1; (B)

nanobiosensor 2 (sample to sample behavior). The laser was applied for 45 sec and laser fluence was set at 45%. Arrow shows the increase of the applied glucose from 0 μM to 40 μM.

In addition, LDI-MS allowed a rapid estimation of inter-daily behavior of nanobiosensors and their inter-daily stability, Figure S13. The clear visible change in LDI-MS profile was established for nanobiosensor after their direct fabrication and after usage during 8 days, Figure S13, A,C. The obtained by LDI-MS dependencies were confirmed by AM investigations, Figure S13, B,D.

Thus, the comparison between LDI-MS chemical profiles and formation of a product specification database makes the standardization of fabrication process of one-step designed nanobiosensors readily possible. General schematic routes for the usage of LDI-MS scanner and the workflow of this approach are summarized in Figure S14.

4. Conclusions

In conclusion, a facile strategy for the standardization of biosensors based upon LDI-MS was presented. A complete characterization of LbL biosensors can be achieved in a non-destructive and informative manner at each fabrication step. Thus, this approach allows both qualitative and quantitative readout of each layer of biosensor. Furthermore, the novel pathways of mediator, polymer and enzyme ionization reported here, represent new routes for quality control during biosensor manufacture. In addition, for the first time, we have shown that LDI-MS scanner can be used to monitor the efficiency of enzyme encapsulation in one-step designed nanobiosensors. Moreover, by means of LDI-MS we visualized and approved the presence of water molecules in one-step hybrid nanobiosensors that can explain their advanced analytical performance. The diversity of capabilities of LDI-MS scanner towards standardization of LbL biosensors and one-step fabricated nanobiosensors can be summarized as follows:

~ non-destructive nanoanalytical tool for the screening of surface functionality;
~ monitoring of surface purity/impurity;
~ monitoring of biochemical homogeneity;
~ imaging of chemical roughness;
~ possibility for sensor-to-sensor and batch-to-batch comparison;
~ evaluation of the chemical composition of the individual layers of LbL biosensors;
~ verification of enzyme and polymer encapsulation in nanobiosensors;
~ can assist the formation of a reliable product specification database;
~ getting qualitative and quantitative information of the end-product;
~ permits the rational design of biosensors/nanobiosensors;
~ rapid run, simple measurement set-up and high throughput;
~ allows completely avoiding the chemical usage and waste generation.

This study is expected to contribute to future discovery, improved design and fine tuning of performance of O-I hybrids, i.e. conventional LbL biosensors and one-step designed nanobiosensors which have broad medical, point-of-care and biotechnological applications. The obtained knowledge on general desorption/ionization mechanism of mediators, polymers and bioreceptors for a wide range of the reagents used in biosensor development will significantly gain the quality test in the production of biosensors with various architectures. However, this would require the formation of a product specification database on the next step. With regards to the future

perspectives, LDI-MS used as a biochemical ´scanner´ can be adapted for the screening of optimal design and validation of wide-range of O-I hybrids, viz. nanozymes and non-enzymatic biosensors.

ACKNOWLEDGEMENTS

This work was a part of the research program funded by the Deutsche Forschungsgemeinschaft (DFG, German Research Foundation, project 427949628).

REFERENCES

(1) Silina, Y. E.; Gernaey, K. V.; Semenova, D.; Iatsunskyi, I. Application of Organic-Inorganic Hybrids in Chemical Analysis, Bio- and Environmental Monitoring. *Applied Sciences (Switzerland)* **2020**, *10* (4). https://doi.org/10.3390/app10041458.

(2) Shi, C. Y.; Deng, C. H. Recent Advances in Inorganic Materials for LDI-MS Analysis of Small Molecules. *Analyst* **2016**, *141* (10), 2816–2826. https://doi.org/10.1039/c6an00220j.

(3) Silina, Y. E.; Volmer, D. A. Nanostructured Solid Substrates for Efficient Laser Desorption/Ionization Mass Spectrometry (LDI-MS) of Low Molecular Weight Compounds. *Analyst* **2013**, *138* (23), 7053–7065. https://doi.org/10.1039/c3an01120h.

(4) Walker, B. N.; Antonakos, C.; Retterer, S. T.; Vertes, A. Metabolic Differences in Microbial Cell Populations Revealed by Nanophotonic Ionization. *Angewandte Chemie - International Edition* **2013**, *52* (13), 3650–3653. https://doi.org/10.1002/anie.201207348.

(5) Myndrul, V.; Viter, R.; Savchuk, M.; Koval, M.; Starodub, N.; Silamiķelis, V.; Smyntyna, V.; Ramanavicius, A.; Iatsunskyi, I. Gold Coated Porous Silicon Nanocomposite as a Substrate for Photoluminescence-Based Immunosensor Suitable for the Determination of Aflatoxin B1. *Talanta* **2017**. https://doi.org/10.1016/j.talanta.2017.07.054.

(6) Tamashevski, A.; Harmaza, Y.; Slobozhanina, E.; Viter, R.; Iatsunskyi, I. Photoluminescent Detection of Human T-Lymphoblastic Cells by ZnO Nanorods. *Molecules (Basel, Switzerland)* **2020**. https://doi.org/10.3390/molecules25143168.

(7) Daniels, J. S.; Pourmand, N. Label-Free Impedance Biosensors: Opportunities and Challenges. *Electroanalysis*. **2007**. https://doi.org/10.1002/elan.200603855.

(8) Wang, J. Glucose Biosensors: 40 Years of Advances and Challenges. *Electroanalysis*. **2001**. https://doi.org/10.1002/1521-4109(200108)13:12<983::aid-elan983>3.0.co;2-%23.

(9) Arlett, J. L.; Myers, E. B.; Roukes, M. L. Comparative Advantages of Mechanical Biosensors. *Nature Nanotechnology*. **2011**. https://doi.org/10.1038/nnano.2011.44.

(10) Semenova, D.; Silina, Y. E. The Role of Nanoanalytics in the Development of Organic-Inorganic Nanohybrids - Seeing Nanomaterials as They Are. **2019**, 12, 1673, https://doi: 10.3390/nano9121673

(11) Semenova, D.; Silina Y.E., Koch, M.; Gernaey, K.V. Sensors for Biosensors: A Novel Tandem Monitoring in a Droplet towards Efficient Screening of Robust Design and Optimal Operating Conditions, *Analyst* **2019**.

https://doi.org/10.1039/c8an02261e.

(12) Semenova, D; Gernaey, K.V.; Morgan, B.; Silina, Y.E. Towards One-Step Design of Tailored Enzymatic Nanobiosensors. *Analyst* **2019**. https://doi.org/10.1039/c9an01745c.

(13) Karyakin, A. A.; Karyakina, E. E.; Gorton, L. On the Mechanism of H2O2 Reduction at Prussian Blue Modified Electrodes. *Electrochemistry Communications* **1999**, *1* (2), 78–82. https://doi.org/10.1016/S1388-2481(99)00010-7.

(14) Pundir, C. S.; Deswal, R.; Narwal, V. Quantitative Analysis of Hydrogen Peroxide with Special Emphasis on Biosensors. *Bioprocess and Biosystems Engineering*. 2018. https://doi.org/10.1007/s00449-017-1878-8.

(15) Koren, K.; Jensen, P.; Kühl, M. Development of a Rechargeable Optical Hydrogen Peroxide Sensor-Sensor Design and Biological Application. *Analyst* **2016**. https://doi.org/10.1039/c6an00864j.

(16) Lu, S. Y.; Chen, Y.; Fang, X.; Feng, X. Hydrogen Peroxide Sensor Based on Electrodeposited Prussian Blue Film. *Journal of Applied Electrochemistry* **2017**. https://doi.org/10.1007/s10800-017-1113-y.

(17) Ricci, F.; Palleschi, G. Sensor and Biosensor Preparation, Optimisation and Applications of Prussian Blue Modified Electrodes. *Biosensors and Bioelectronics*. 2005. https://doi.org/10.1016/j.bios.2004.12.001.

(18) Pauk, V.; Havlíček, V.; Papoušková, B.; Sulovský, P.; Lemr, K. Simultaneous Identification of Historical Pigments Prussian Blue and Indigo in Paintings by Electrospray Mass Spectrometry. *Journal of Mass Spectrometry* **2013**, *48* (8), 927–930. https://doi.org/10.1002/jms.3228.

(19) Kuckova, S.; Hynek, R.; Němec, I.; Kodiček, M.; Jehlička, J. Critical Comparison of Spectrometric Analyses of Non-Mineral Blue Dyes and Pigments Used in Artworks. *Surface and Interface Analysis* **2012**, *44* (8), 963–967. https://doi.org/10.1002/sia.4828.

(20) Merino, J. P.; Serna, S.; Criado, A.; Centeno, A.; Napal, I.; Calvo, J.; Zurutuza, A.; Reichardt, N.; Prato, M. Mass Spectrometry of Carbohydrate-Protein Interactions on a Glycan Array Conjugated to CVD Graphene Surfaces. *2D Materials* **2020**. https://doi.org/10.1088/2053-1583/ab6030.

(21) Liu, Y.; Liu, J.; Deng, C.; Zhang, X. Graphene and Graphene Oxide: Two Ideal Choices for the Enrichment and Ionization of Long-Chain Fatty Acids Free from Matrix-Assisted Laser Desorption/Ionization Matrix Interference. *Rapid Communications in Mass Spectrometry* **2011**. https://doi.org/10.1002/rcm.5218.

(22) Liang, K.; Gao, H.; Gu, Y.; Yang, S.; Zhang, J.; Li, J.; Wang, Y.; Wang, Y.; Li, Y. Graphene Oxide Aggregate-Assisted LDI-MS for the Direct Analysis of Triacylglycerol in Complex Biological Samples. *Analytica Chimica Acta* **2018**. https://doi.org/10.1016/j.aca.2018.07.049.

(23) Liu, C. W.; Chien, M. W.; Su, C. Y.; Chen, H. Y.; Li, L. J.; Lai, C. C. Analysis of Flavonoids by Graphene-Based Surface-Assisted Laser Desorption/Ionization Time-of-Flight Mass Spectrometry. *Analyst* **2012**. https://doi.org/10.1039/c2an36155h.

(24) Chang, W. C.; Huang, L. C. L.; Wang, Y. S.; Peng, W. P.; Chang, H. C.; Hsu, N. Y.; Yang, W. Bin; Chen, C. H. Matrix-Assisted Laser Desorption/Ionization (MALDI) Mechanism Revisited. *Analytica Chimica Acta* **2007**, *582* (1), 1–9. https://doi.org/10.1016/j.aca.2006.08.062.

(25) Nishikaze, T.; Okumura, H.; Jinmei, H.; Amano, J. Correlation between Sweet Spots of Glycopeptides and Polymorphism of the Matrix Crystal in MALDI Samples. *Mass Spectrometry* **2012**. https://doi.org/10.5702/massspectrometry.a0006.

(26) Ruiz-Bermejo, M.; Rogero, C.; Menor-Salván, C.; Osuna-Esteban, S.; Martín-Gago, J. Á.; Veintemillas-Verdaguer, S. Thermal Wet Decomposition of Prussian Blue: Implications for Prebiotic Chemistry. *Chemistry and Biodiversity* **2009**, *6* (9), 1309–1322. https://doi.org/10.1002/cbdv.200900024.

(27) Silina, Y. E.; Koch, M.; Volmer, D. A. Influence of Surface Melting Effects and Availability of Reagent Ions on LDI-MS Efficiency after UV Laser Irradiation of Pd Nanostructures. *Journal of Mass Spectrometry* **2015**, *50* (3).

https://doi.org/10.1002/jms.3564.

(28) Feng, M.; Qu, R.; Wei, Z.; Wang, L.; Sun, P.; Wang, Z. Characterization of the Thermolysis Products of Nafion Membrane: A Potential Source of Perfluorinated Compounds in the Environment. *Scientific Reports* **2015**, *5*, 1–8. https://doi.org/10.1038/srep09859.

(29) Pyatenko, A.; Wang, H.; Koshizaki, N.; Tsuji, T. Mechanism of Pulse Laser Interaction with Colloidal Nanoparticles. *Laser and Photonics Reviews*. **2013**. https://doi.org/10.1002/lpor.201300013.

(30) Si, P.; Huang, Y.; Wang, T.; Ma, J. Nanomaterials for Electrochemical Non-Enzymatic Glucose Biosensors. *RSC Advances*. 2013. https://doi.org/10.1039/c2ra22360k.

(31) Park, S.; Boo, H.; Chung, T. D. Electrochemical Non-Enzymatic Glucose Sensors. *Analytica Chimica Acta*. **2006**. https://doi.org/10.1016/j.aca.2005.05.080.

(32) Jia, W.; Bandodkar, A. J.; Valdés-Ramírez, G.; Windmiller, J. R.; Yang, Z.; Ramírez, J.; Chan, G.; Wang, J. Electrochemical Tattoo Biosensors for Real-Time Noninvasive Lactate Monitoring in Human Perspiration. *Analytical Chemistry* **2013**. https://doi.org/10.1021/ac401573r.

(33) Kim, Y. R.; Bong, S.; Kang, Y. J.; Yang, Y.; Mahajan, R. K.; Kim, J. S.; Kim, H. Electrochemical Detection of Dopamine in the Presence of Ascorbic Acid Using Graphene Modified Electrodes. *Biosensors and Bioelectronics* **2010**. https://doi.org/10.1016/j.bios.2010.02.031.

(34) Khan, A.; Khan, A. A. P.; Asiri, A. M.; Rub, M. A.; Azum, N.; Rahman, M. M.; Khan, S. B.; Ghani, S. A. A New Trend on Biosensor for Neurotransmitter Choline/Acetylcholine - An Overview. *Applied Biochemistry and Biotechnology* **2013**. https://doi.org/10.1007/s12010-013-0099-0.

(35) Klibanov, A. Why Are Enzymes Less Active in Organic Solvents than in Water? *Trends in Biotechnology* **1997**. https://doi.org/10.1016/S0167-7799(97)01013-5.

(36) Zaks, A.; Klibanov, A. M. The Effect of Water on Enzyme Action in Organic Media. *The Journal of biological chemistry* **1988**.

(37) Itoh, Y.; Ohashi, Y.; Shibue, T.; Hayashi, A.; Maki, S.; Hirano, T.; Niwa, H. Reduction in Desorption Mass Spectrometry: Multiple Protonation on Flavins without Charge Increment. *Journal of the Mass Spectrometry Society of Japan* **2002**, *50* (2), 52–57. https://doi.org/10.5702/massspec.50.52.

626 # Graphical abstract

627

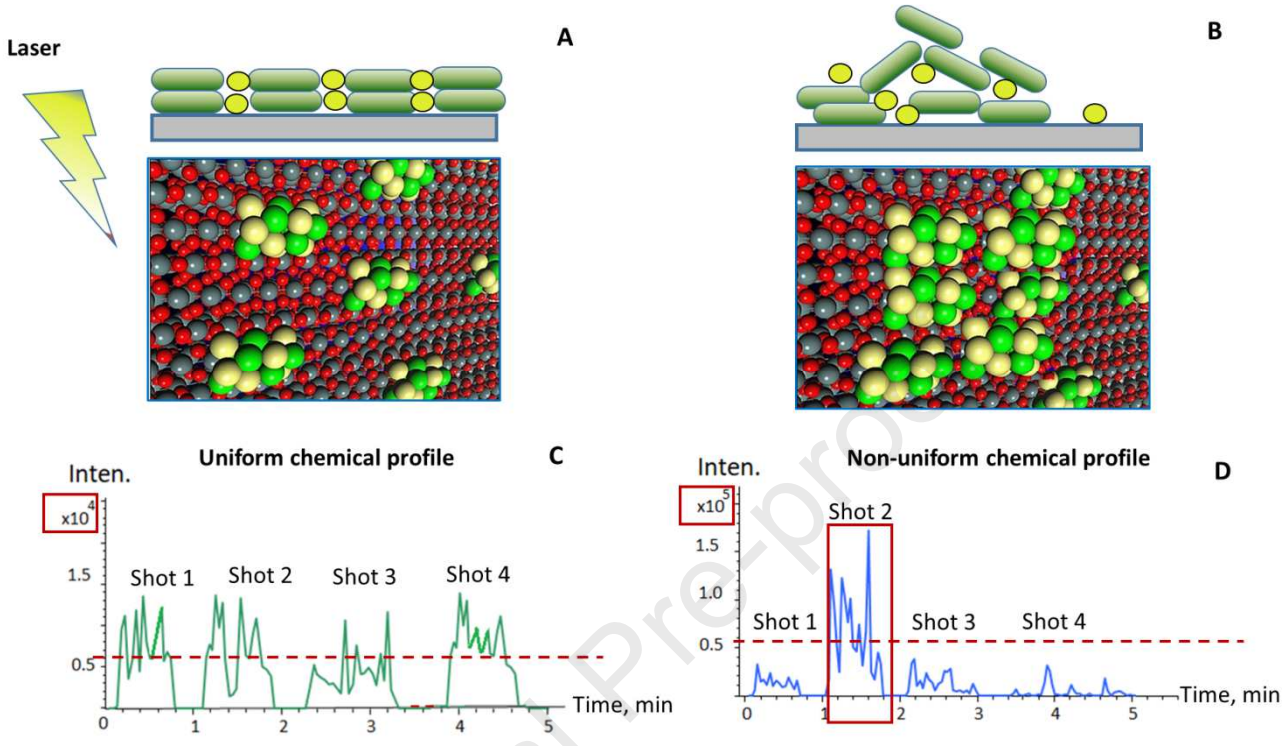

628

1. LDI-MS-based approach applied for the standardization of amperometric biosensors was optimized.

2. Specific ionization pathways of mediators, polymers and enzymes for robust quality control during biosensor manufacture were established.

3. LDI-MS can be used to monitor and ensure the encapsulation of enzymes in one-step designed nanobiosensors.

4. The approach assesses the synthesis quality of LbL-biosensors and one-step designed nanobiosensors.

5. The assay allows monitoring for batch-to-batch and intra- and interring- day changes in biosensor´s function and behavior.

Declaration of interests

☒ The authors declare that they have no known competing financial interests or personal relationships that could have appeared to influence the work reported in this paper.

☐The authors declare the following financial interests/personal relationships which may be considered as potential competing interests:

Dr. Yuliya E. Silina
17.07.2020